Optimal transport exponent in spatially embedded networks

G. Li,[1] S. D. S. Reis,[2] A. A. Moreira,[2] S. Havlin,[1,3] H. E. Stanley,[1] and J. S. Andrade, Jr.[2]
[1]*Center for Polymer Studies, Boston University, Boston, Massachusetts 02215, USA*
[2]*Departamento de Física, Universidade Federal do Ceará, 60451-970 Fortaleza, Ceará, Brazil*
[3]*Department of Physics, Bar-Ilan University, 52900 Ramal-Gab, Israel*
(Received 30 August 2012; published 18 April 2013)

The imposition of a cost constraint for constructing the optimal navigation structure surely represents a crucial ingredient in the design and development of any realistic navigation network. Previous works have focused on optimal transport in small-world networks built from two-dimensional lattices by adding long-range connections with Manhattan length r_{ij} taken from the distribution $P_{ij} \sim r_{ij}^{-\alpha}$, where α is a variable exponent. It has been shown that, by introducing a cost constraint on the total length of the additional links, regardless of the strategy used by the traveler (independent of whether it is based on local or global knowledge of the network structure), the best transportation condition is obtained with an exponent $\alpha = d + 1$, where d is the dimension of the underlying lattice. Here we present further support, through a high-performance real-time algorithm, on the validity of this conjecture in three-dimensional regular as well as in two-dimensional critical percolation clusters. Our results clearly indicate that cost constraint in the navigation problem provides a proper theoretical framework to justify the evolving topologies of real complex network structures, as recently demonstrated for the networks of the US airports and the human brain activity.

DOI: 10.1103/PhysRevE.87.042810 PACS number(s): 89.75.Hc

I. INTRODUCTION

In recent years, complex weblike structures have been the subject of intensive research in several fields, including those focusing on social relationships, biological resources, and transportation systems [1–7]. The topological features of these systems, which go beyond the standard regular lattice geometry, have been described in terms of complex network structures. In this way, the theory of random graphs as well as concepts such as small worldliness and scale freeness have been consistently used to characterize and classify the diverse complex networks found in nature [8–13], providing interesting insights about their underlying structure and functionality. Generally speaking, the geometrical features of complex networks are not necessarily associated with or restricted to a given topological dimension in space. However, a large number of real transport networks can be geographically represented or spatially embedded [14–18], such as the US airport network [19], networks of streets and highways [20], physical systems [21], mobile agents [22], and also the network of activity in the brain [23,24].

In science, nature, and technology, the transport of information, energy, or even people can be optimized by adding long-range connections (shortcuts) to an underlying geographical network. In recent studies [25,26], it has been shown that the optimal design of transport networks can be associated with the presence of special critical correlations between the local structure and the long-range connections, added in such a way as to generate gradients that permit the information to flow efficiently from source to target in the network. In several real systems, however, transport is usually constrained by some involved cost. In a subsequent study [27], it has been shown that, without loss of generality, transport with local and global knowledge on a square lattice with cost limitation on the additional links can be optimized through the inclusion of long-range connections between pairs of nodes following a probability distribution that decays as a power law of their Manhattan distance, namely, the distance counted as the number of connections separating nodes in the regular lattice. Efficient transport is then obtained when the exponent α of the power-law distribution is tuned to 3 for a two-dimensional lattice, in sharp contrast with the previous results for unconstrained local [25,26] and global [28] navigation, where the optimal values are $\alpha = 2$ and 0, respectively. Considering the results for a one-dimensional ring and a two-dimensional lattice, it is then conjectured that optimal transport with cost constrained is achieved when $\alpha = \alpha_e = d + 1$ for a d-dimensional lattice. Subsequently, power-law distributions of long-range connections on geographical networks have also been used to study navigation and other types of processes [20,29–34]. Moreover, as suggested in Ref. [27], the value of $\alpha \approx 3$ for airline networks reported by Bianconi *et al.* [19] may be due to optimizing the transportation system. Furthermore, recent studies by Gallos *et al.* measured empirically α in the brain and found $\alpha = d_f + 1 \approx 3$, which may suggest that the brain is optimizing connections with a cost constraint [23,24].

In this work, we propose a real-time algorithm for efficient study of the global navigation. Using this algorithm, simulation results could be obtained for large system sizes, up to the order of 10^9 nodes. This is carried out by memorizing only the neighbors of a particular node at each time step of the algorithm. Initially, optimal exponents have been obtained using this algorithm, reproducing previous numerical estimates of both unconstrained and constrained global navigation for one and two dimensions [25–29]. In addition, we present here results of simulations for three-dimensional global navigation and constrained global navigation processes on a fractal lattice of dimension d_f, reinforcing the conjectured optimal navigation exponent $\alpha_e = d + 1$. The paper is organized as follows. In Sec. II we present the basic model we use to study the navigation on spatially embedded networks, namely, the Kleinberg model [25]. In Sec. III the real-time algorithm for global navigation on spatially embedded networks is

introduced. In Sec. IV the conjecture previously reported in the literature for the optimal navigation with global knowledge and without cost limitation is further supported for one-, two-, and three-dimensional systems. In addition, results from simulations with cost limitation for one, two, and three dimensions, as well as for two-dimensional percolation lattices, are presented and discussed. In Sec. V we present an analytic argument for the scaling behavior. We leave the final summary for Sec. VI.

II. NAVIGATION WITH LOCAL INFORMATION

Using local information and a decentralized algorithm, the problem of efficient navigation in small-world networks was recently studied by Kleinberg [25]. Figure 1 shows a regular two-dimensional square lattice with $N = L \times L$ nodes, where L is the linear size of the lattice. Accordingly, each node i has a random long-range connection to a node j with probability $P(r_{ij}) \sim r_{ij}^{-\alpha}$, where r_{ij} is the lattice (Manhattan) distance between nodes i and j. This model follows the small-world paradigm, i.e., it is rich in short-range connections, but has only a few long-range connections. The optimal delivery time by a decentralized algorithm based on the local information occurs when the exponent $\alpha = 2$ [25].

The probability $P(r_{ij})$ that nodes i and j will have a long-range connection can be mapped on a density distribution $p(r)$, where $r = r_{ij}$. The number of nodes separated by a lattice distance r from a given node in a d-dimensional lattice is proportional to r^{d-1} (see Fig. 1). Thus we have

$$p(r) \sim r^{-\alpha} r^{d-1}. \tag{1}$$

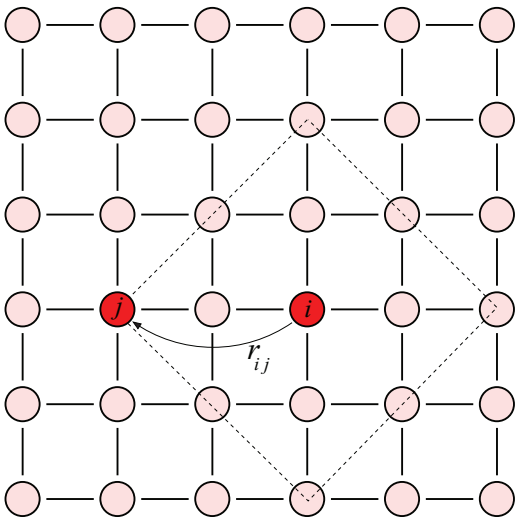

FIG. 1. (Color online) Two-dimensional square lattice with long-range connections. Each node has four short-range connections to its nearest neighbors. A long-range connection is added to a randomly chosen node i with probability proportional to $r^{-\alpha}$. Here $r = 2$, there are eight nodes (on the dashed square box) with the same lattice distance r to node i, and we randomly choose the node j from these eight nodes to be connected to node i.

The normalization factor of Eq. (1) scales as

$$\int_1^L r^{-\alpha} r^{d-1} dr \sim \begin{cases} L^{d-\alpha}, & \alpha < d \\ \ln L, & \alpha = d \\ (\alpha - d)^{-1}, & \alpha > d, \end{cases} \tag{2}$$

where $L = N^{1/d}$.

In order to improve the transport property of a lattice network, it is not necessary to assign every node a long-range connection, which would be a high-cost strategy. Instead, we assign a long-range connection to a small fraction of randomly selected nodes. This leads to a dramatic improvement in the transport properties of the network, but at a much lower cost. This model can be generated using the following steps.

(i) A regular d-dimensional lattice with N nodes is created with each node connected to its $2d$ nearest neighbors.

(ii) A node i is randomly selected from the total N nodes to receive a long-range connection. The length of the long-range connection r is randomly generated using Eqs. (1) and (2).

(iii) Another node j is also randomly selected from those nodes with the same lattice distance r to node i. We then connect node i and node j. For example, Fig. 1 shows eight nodes (on the dashed square box) that have the same lattice distance to node i ($r = 2$). We randomly take node j from these eight nodes and connect it to node i.

(iv) Repeat steps (ii) and (iii) until the total number of long-range connections N_l reaches a preset value, e.g., 10% of the total number of nodes N.

III. REAL-TIME ALGORITHM FOR GLOBAL NAVIGATION

In many real-world optimal navigation problems, one has access to global information when designing the optimal transport network. With global information, between any two randomly selected nodes a and b, we can compute the shortest path length ℓ_{ab}, which is in sharp contrast with the delivery time based on local information. For the specific model, i.e., the Kleinberg model [25] introduced in Sec. II, we will show in the next section that ℓ follows approximately a Gaussian distribution. Since almost all values lie close to the average value in a Gaussian distribution, the average shortest path length $\langle \ell \rangle$ of the Kleinberg model is thus the most important parameter to evaluate the overall shortest path length between each pair of nodes, namely, transport efficiency of the entire network.

The usual method of calculating $\langle \ell \rangle$ is first to build the model with long-range connections and then measure the shortest path length ℓ for every pair of nodes. This method is fast and effective for small systems, however, given the present-day computer resources, it is neither practical nor efficient to prebuild such a big system and then add long-range connections.

Hence we introduce a real-time algorithm to calculate $\langle \ell \rangle$ for large systems, which gives us the same results as the common method previously described, but much faster. To evaluate $\langle \ell \rangle$ for a network, the usual procedure is to calculate the shortest path length for every pair of nodes. If we have many realizations of a network, however, we can randomly pick one pair of nodes in one realization and calculate ℓ of this

pair. Then, in another realization, we randomly pick another pair of nodes and calculate ℓ again. After a large number of realizations, we are then able to determine $\langle \ell \rangle$. Since for every realization the network is created by using the same parameters, $\langle \ell \rangle$ from many different realizations reflects the result from different pairs of nodes in a single network.

For a single realization of the real-time algorithm, it is not necessary to create the entire network. Starting from a randomly selected node a, we generate its neighbors in real time (time step). For example, in a square lattice, node a always has four nearest neighbors (or $2d$ nearest neighbors on a d-dimensional lattice); if node a is on the boundary, we generate its neighbors using a periodic boundary condition. After that, we consider the additional long-range connections of node a, the one that it receives according to step (ii), and the others that eventually start from another node, according to step (iii). As long as we have all the available neighbors of node a (including connections to both the nearest and long-range neighbors), we record and classify them as shell-1 nodes, meaning that they are one link apart from node a. After that, we generate all the neighbors of the shell-1 nodes not generated yet and classify them as shell-2 nodes. We repeat this process until we reach the destination node b, which is also randomly selected. We count the number of steps from node a to node b during this process. In this way, we find ℓ_{ab} between nodes a and b. We repeat many realizations to find the average $\langle \ell \rangle$, until we generate a smooth curve $\langle \ell \rangle$ vs α for different values of α.

A crucial step of this algorithm is when we consider the additional long-range connections of node a. When we add long-range connections to the network we always randomly select two nodes with the lattice distance r, thus the number of additional long-range connections k_l for each node obeys a Poisson distribution

$$f(k_l) = \frac{\lambda^{k_l} e^{-\lambda}}{k_l!}, \tag{3}$$

where λ is the average number of long-range connections for each node and is calculated as

$$\lambda = \langle k_l \rangle = \frac{2N_l}{N}, \tag{4}$$

where N_l is the total number of long-range connections, which can be a preset value.

Using the Poisson distribution (3), we generate the number of long-range connections k_l for node a. It must be noted that k_l can be greater than one, which means we do not limit the number of long-range connections for each node. This is a little different from the original model of Kleinberg in which each node has one long-range connection. From Eqs. (1) and (2) we assign r to each long-range connection of node a. Finally, as described in step (iii), we choose all the long-range neighbors for node a.

In this real-time algorithm, we do not build the entire network, but only generate the neighbors needed for each step. This algorithm saves computer resources and, as we shall see later, produces exactly the same results as those from the more usual method of building the entire network. This real-time algorithm makes the simulation of very large systems possible (e.g., 10^9 nodes).

IV. RESULTS AND DISCUSSION

We note that when $\langle \ell \rangle$ is based on the global information of the network it does not demonstrate the uniqueness of the navigation based on local information described by Kleinberg. In this case, the optimal $\langle \ell \rangle$ is achieved at $\alpha_e = 0$ [28], which can be understood from a simple analysis. When $\alpha = 0$, the length of the long-range connections does not depend on the distance and thus the process of adding long-range connections is simply the same as the procedure used to create a Watts-Strogatz network [11] or even an Erdős-Rényi network [8,9]. In this situation, the average shortest path length scales as a logarithm function of the network size $\langle \ell \rangle \sim \ln N$.

Figure 2 shows $\langle \ell \rangle$ for three different lattices ($d = 1$, 2, and 3) with the same linear size $L = 1000$, in which a fixed fraction (10%) of nodes receive long-range connections. We find that the optimal $\langle \ell \rangle$ indeed emerges at $\alpha_e = 0$. Moreover, when $\alpha < d$ (for $d = 1$, 2, and 3), $\langle \ell \rangle$ appears almost the same as the results for $\alpha = 0$, which means in this regime $\langle \ell \rangle \sim \ln N$, and that the transport property behaves as small-world networks (see also Ref. [28,34]).

In real-world situations, however, the financial cost of adding links always plays an important role when aiming to improve the transport in an existing network. Consider, for example, the case of an existing network with a transport efficiency that needs improvement [35]. Creating a large number of long-range connections is not feasible because the available resources are limited. This cost limitation can be modeled by fixing the total length of additional long-range connections to a certain number $\Lambda \equiv \sum r_{ij}$. We further assume that the total cost Λ will be proportional to the size N of the network, i.e., $\Lambda = AN$, where A is a constant [27]. This assumption is justified since bigger systems should obtain proportionally larger budgets for improvement. Moreover, the total length of the links in the original lattice is proportional to N (number of nodes).

When the total cost is fixed, there is a trade-off between the length and the number of long-range connections N_l. If the total cost is fixed at $\Lambda = AN = AL^d$, the available number of

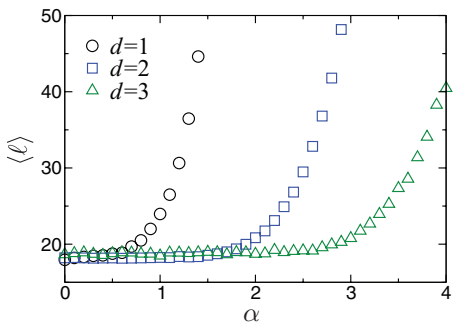

FIG. 2. (Color online) A fraction of 10% of nodes in a regular d-dimensional ($d = 1$, 2, and 3) lattice with linear size $L = 1000$ are randomly selected to receive long-range connections with different α. As seen, the optimal $\langle \ell \rangle$ is achieved for $\alpha = 0$. The results are averaged over 4000 realizations for each network. Note that when α increases above the value of d, $\langle \ell \rangle$ increases dramatically. For the dependence of $\langle \ell \rangle$ on L for different α, see Refs. [28,32,34].

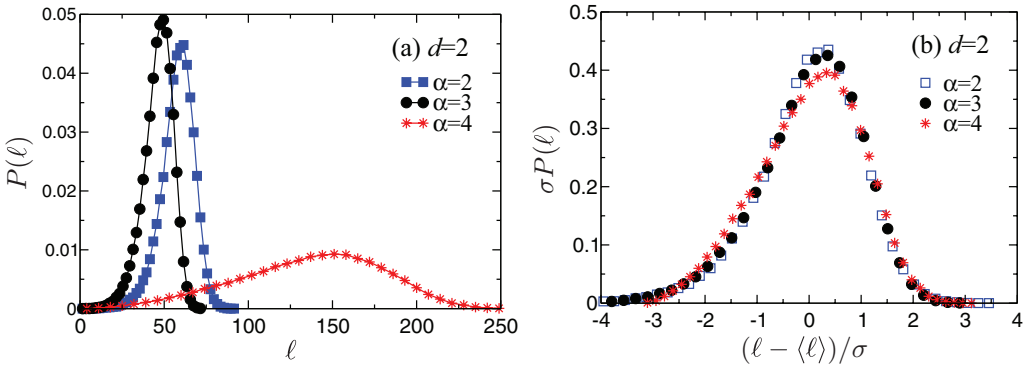

FIG. 3. (Color online) (a) Distribution and (b) normalized distribution of the shortest path length ℓ for a two-dimensional lattice ($L = 1000$) with additional long-range connections where the total length Λ of the added long-range connections is limited to $N = L^2$. Note the nonmonotonic behavior with respect to α. For $\alpha = d + 1 = 3$ the location of the peak of the distribution is the smallest. In (b), $\langle \ell \rangle$ is the mean ℓ and σ is the standard deviation for each curve. We sampled 100 000 network realizations for each α.

long-range connections will be

$$N_l = \Lambda / \langle r \rangle, \tag{5}$$

where $\langle r \rangle$ is the average length of long-range connections, which can be calculated from (1) for a given α as

$$\langle r \rangle \sim \int_1^L r^{d-\alpha} dr \sim \begin{cases} L, & \alpha < d \\ L/\ln L, & \alpha = d \\ L^{d+1-\alpha}, & d < \alpha < d+1 \\ \ln L, & \alpha = d+1 \\ 1, & \alpha > d+1. \end{cases} \tag{6}$$

Note that in Eq. (6), $\langle r \rangle$ decreases and N_l increases when α increases. When α is small ($\alpha \leqslant d$), $\langle r \rangle \sim L$, and $N_l = \Lambda / \langle r \rangle \sim L^{d-1}$, only a small fraction (in fact, zero fraction in the limit $L \to \infty$) of nodes are needed to have long-range connections in order to improve the transport of the network. When $\alpha > d + 1$, however, a large number of long-range connections are available ($N_l \sim L^d$) to improve the transport of the network, but each long-range connection is short; thus these long-range connections do not efficiently improve transport. Thus the intermediate regime of α can be expected to be useful and optimize the transport on the network, i.e., $d < \alpha \leqslant d + 1$.

Figure 3(a) shows the distribution $P(\ell)$ of shortest path length ℓ for different α on a two-dimensional lattice with additional long-range connections of total length $N = L^2$. Note that $P(\ell)$ follows an approximate Gaussian distribution for different α. Consequently, since $\langle \ell \rangle$ has its minimum value when $\alpha = d + 1 = 3$, the optimal navigation is achieved at that α value. Figure 3(b) shows the normalized distribution $P(\ell)$ for different α. The different curves in Fig. 3(a) approximately collapse to a single curve when scaled appropriately.

We study additional quantitative information about the transport properties of the network by performing extensive simulations for different system sizes N and different values of α. We first focus on identifying the optimal transport conditions on regular lattices, i.e., $d = 1$, 2, and 3. In each case, we simply add long-range connections to the regular lattice. The procedure is almost the same as in the Kleinberg navigation model, except that in step (iv) we stop adding the long-range connections when the total length of long-range connections $\sum r_{ij}$ reaches a preset value $\Lambda = AN$, instead of a fixed number of long-range connections. After that, we calculate the average shortest path $\langle \ell \rangle$ over all realizations of pairs of nodes.

From the results in Figs. 4(a)–4(c), we see the presence of a minimum $\langle \ell \rangle$ for different system sizes at the same value of the exponent $\alpha = d + 1$, when $N \to \infty$. Thus, based on the global knowledge of the network structure, the most efficient navigation occurs at $\alpha_e = d + 1$.

Thus far for the Kleinberg model with global information available, the transport property of the network can be presented by the average shortest path length $\langle \ell \rangle$, which changes with exponent α and reaches a minimal value where optimal transport occurs. After we introduce cost to each long-range link, the cost of total long-range connection Λ becomes a crucial parameter to affect the optimal transport exponent α_e. If Λ is not constrained, i.e., $\Lambda \to \infty$, from Fig. 2, the optimal transport occurs at $\alpha = 0$; with cost constrained $\Lambda \sim N$, α_e goes to $d + 1$. Therefore, in the intermediate regime, there exists a crossover between $\alpha_e = 0$ and $\alpha_e = d + 1$. It must be noted that the optimal delivery time without cost constrained studied by Kleinberg occurs at $\alpha = d$, which is based on local information with a decentralized algorithm [25]. We study the average shortest path length $\langle \ell \rangle$ based on the global information with cost constrained and find that the minimal $\langle \ell \rangle$ occurs at $\alpha = d + 1$. We also found that the optimal delivery time with cost constrained based on local information occurs at $\alpha = d + 1$, as in the previous work [27].

To further test the optimal navigation condition $\alpha = d + 1$ with cost constrained, we plot $\langle \ell \rangle$ vs L for different α. Figures 5(a)–5(c) clearly show that for $\alpha \neq d + 1$ the shortest path length $\langle \ell \rangle$ follows a power law with L. For $\alpha = d + 1$, $\langle \ell \rangle$ follows a power law with a smaller exponent when $d = 1$ [Fig. 5 (a)] and it appears to be less than a power law for $d > 1$ [Figs. 5(b) and 5(c)].

Figures 4(d) and 5(d) show the analogous optimal navigation results when the substrate is a fractal. Specifically, the fractal is generated from an original two-dimensional regular lattice. We randomly remove the nodes with a probability $1 - p = q$. We increase q from 0 until a critical percolation occurs [36,37]. In this critical condition $q = q_c \cong 0.4$ a giant cluster extends from top to bottom and from left to right across

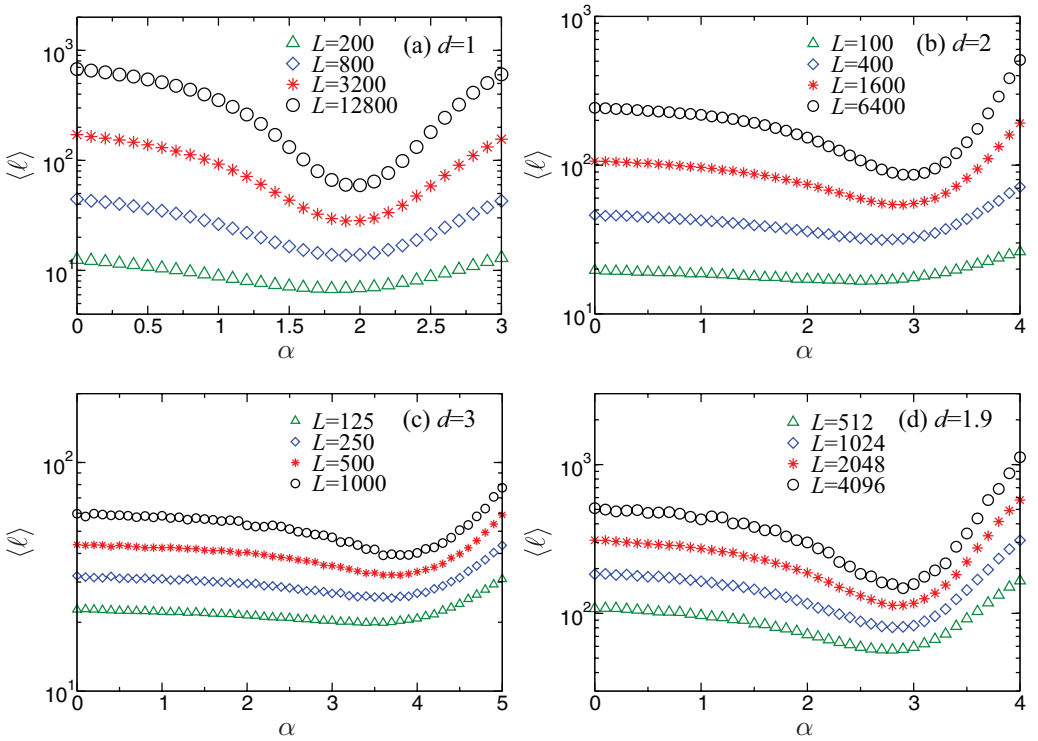

FIG. 4. (Color online) Average shortest path length $\langle \ell \rangle$ as a function of α for (a) one-, (b) two-, and (c) three-dimensional lattices and (d) a fractal ($d = d_f \cong 1.9$) with additional long-range connections taken from the power-law distribution (1) as a function of α. The total length Λ of the added long-range connections is limited to $10N$ for the one-dimensional lattice, N for the two- and three-dimensional lattices, and N_f for the fractal. The plots suggest that the optimal shortest path length is achieved at $\alpha = d + 1$ for regular lattices and $\alpha = d_f + 1$ for the fractal. Note that (b) is similar to Fig. 3 in Ref. [27] but with larger system sizes. The results are averaged over 4000 realizations for the three smaller L and 400 realizations for the largest L.

the lattice, which is a fractal. The dimension of this giant cluster is $d_f \cong 1.9$. In Ref. [26] it is shown that for local navigation and without constraints on total length, the optimal transport is for $\alpha = d_f$. In order to improve the transport with global knowledge of this fractal, we append additional long-range connections to the cluster using the same procedure as in a two-dimensional regular lattice. The difference here is that the total length of long-range connections is fixed to be AN_f, where N_f is the number of nodes in the giant component of the fractal, which can be calculated as $N_f = L^{d_f}$. From Figs. 4(d) and 5(d), we see that optimal navigation occurs at $d_f + 1 \cong 2.9$ when $N \to \infty$. We also test another fractal lattice, i.e., the Sierpinski carpet [38], with $d_f = 1.89$ and find that the optimal navigation is achieved at $d_f + 1 \cong 2.89$ when $N \to \infty$. Note that the real-time algorithm cannot be used on these critical percolation lattices because the shortest path length is calculated on the giant cluster, which must be prebuilt up.

Figure 5(a) suggests that in a one-dimensional lattice $\langle \ell \rangle$ always follows a power-law dependence as a function of system sizes. For $d > 1$, as seen in Figs. 5(b) and 5(c), however, $\langle \ell \rangle$ scales as a power law with the system linear size L for all values of α except for $\alpha = d + 1$, for which the scaling seems to be less than a power law. For $d > 1$, we test two possible forms for $\langle \ell \rangle$ vs L: (i) a power law and (ii) a logarithmic law. Figure 6(a) shows the successive slopes δ_s obtained from $\ln\langle \ell \rangle$ vs $\ln L$ for $d = 2$, testing whether $\langle \ell \rangle$ follows a power law or not. Here we assume $\langle \ell \rangle \sim L^{\delta_s}$ and see that δ_s remains approximately constant when $\alpha \neq d + 1$, but decreases when $\alpha = d + 1 = 3$. This suggests that $\langle \ell \rangle$ follows a power law only when $\alpha \neq d + 1$. Similar results have been obtained for $d = 3$ and $d = d_f$. We next assume that $\langle \ell \rangle$ vs L follows a logarithmic law with exponent γ_s, i.e., $\langle \ell \rangle \sim \ln^{\gamma_s} L$. In Fig. 6(b) we plot the data assuming this function in a double logarithmic plot. As can be seen, apart from the case $\alpha = 3$, which fits quite well as a straight line (with $\gamma_s \cong 2.5$), for the other values of α, $\langle \ell \rangle$ increases faster. Indeed, we plot in Fig. 6(c) the successive slopes γ_s obtained from the plot of $\ln\langle \ell \rangle$ vs $\ln\ln L$ for $d = 2$ [Fig. 6(b)]. We see that γ_s keeps almost a constant value ($\gamma_s \cong 2.5$) when $\alpha = d + 1 = 3$, but it increases when $\alpha \neq d + 1$. This suggests that $\langle \ell \rangle$ follows a power law of a logarithmic dependence when $\alpha = d + 1$. Similar results have been obtained for $d = 3$ and $d_f = 1.9$.

V. ANALYTIC ARGUMENTS

Besides the support from simulation results, we present analytic arguments suggesting that for $N \to \infty$ the optimal navigation is achieved for $\alpha = d + 1$. Figure 5(a) shows the one-dimensional case in which the scaling of $\langle \ell \rangle$ with L is a power law for different α and that the power law is smallest when $\alpha = 2$. Li *et al.* [30] provide an exact solution for the optimal navigation with a total cost restriction for the one-dimensional case. They conclude that for $d = 1$, the optimal navigation occurs at $\alpha = 2$ when $N \to \infty$.

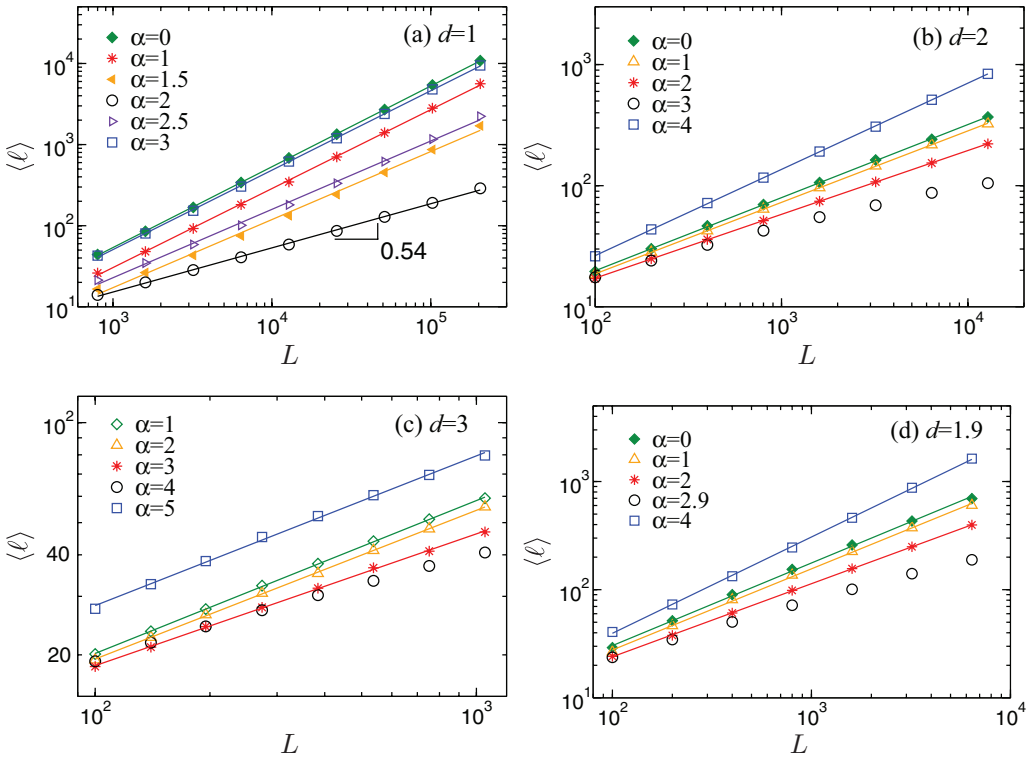

FIG. 5. (Color online) Average shortest path length $\langle \ell \rangle$ as a function of system linear size L with different α for (a) one-, (b) two-, (c) and three-dimensional lattices and (d) a fractal ($d_f \cong 1.9$) with additional long-range connections taken from the power-law distribution (1). The total length Λ of the added long-range connections is limited to $10N$ for the one-dimensional lattice, N for the two- and three-dimensional lattices, and N_f for the fractal. The plots suggest that the optimal shortest path length is achieved at $\alpha = d + 1$ for regular lattices and $\alpha = d_f + 1$ for the fractal. For $d = 1$, the slope of the fitting line $\delta_s \cong 0.54$ for $\alpha = d + 1 = 2$, $\delta_s \approx 0.84$ for $\alpha = 1.5$ and 2.5, and $\delta_s \approx 1$ for $\alpha = 0$, 1, and 3. For $d = 2$, $\delta_s \approx 0.60$ for $\alpha = 0$ and 1 and $\delta \cong 0.71$ for $\alpha = 4$; however, for $\alpha = d + 1 = 3$, $\langle \ell \rangle$ seems to follow a weaker dependence from a power law, more likely a logarithmic law [see Fig. 6 (b)]. For $d = 3$, $\delta_s \approx 0.46$ for $\alpha = 0,1$, and 2, $\delta_s \cong 0.40$ for $\alpha = 3$, and $\delta_s \cong 0.45$ for $\alpha = 5$; however, for $\alpha = d + 1 = 4$, $\langle \ell \rangle$ seems to follow a logarithmic law. For $d = 1.9$, $\delta_s \approx 0.75$ for $\alpha = 0$ and 1 and $\delta \cong 0.89$ for $\alpha = 4$; however, for $\alpha = d_f + 1 = 2.9$, $\langle \ell \rangle$ seems to follow a logarithmic law. The results are averaged over 4000 realizations for each α for $d = 1$,2, and 3 and 1000 realizations for $d = 1.9$.

Next, we suggest a simple analysis showing that for $d > 1$, $\alpha = d + 1$ is indeed the only case for which a logarithmic scaling of $\langle \ell \rangle$ with L can occur, while for $\alpha \neq d + 1$ a power law with L must hold. For a fixed total cost $\Lambda = AL^d$, the density of long-range connections is defined as $\rho = N_l/N$, where N_l is the available number of long-range connections in the lattice. From Eq. (5) and $\Lambda = AN$ we find that $\rho = A\langle r \rangle^{-1}$. From Eq. (6) it follows that for $d \leqslant \alpha < d + 1$, $\rho \sim L^{\alpha - d - 1}$ and, for $\alpha < d$, $\langle r \rangle \sim L$, leading to $\rho \sim L^{-1}$. So when $\alpha < d + 1$, the density ρ of long-range connections decreases as a power law with L. As a consequence of this power-law decrease in density, $\langle \ell \rangle$ must increase as a power of L. To verify this, we

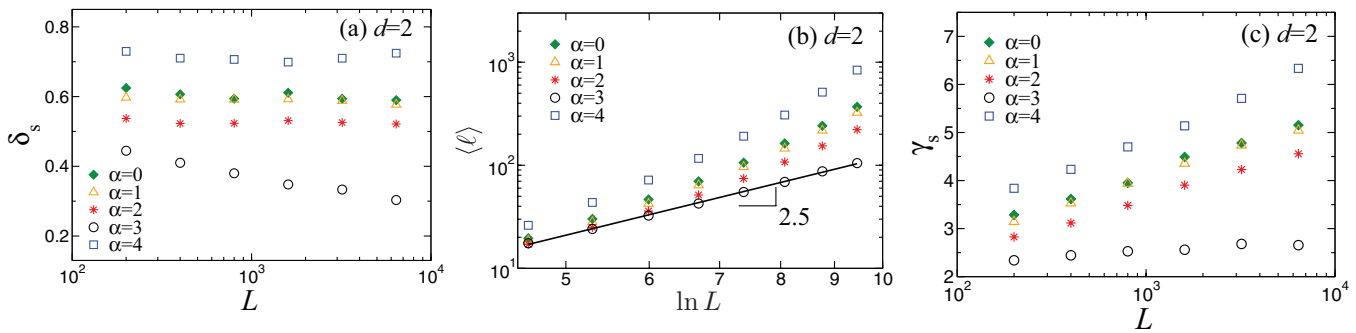

FIG. 6. (Color online) Successive slopes for $d = 2$ of (a) δ_s obtained from $\ln\langle \ell \rangle$ vs $\ln L$ [of Fig. 5(b)], (b) $\langle \ell \rangle$ as a function of $\ln L$ in a double logarithmic plot, and (c) γ_s obtained from $\ln\langle \ell \rangle$ vs $\ln\ln L$ taken from (b). The total length Λ of the added long-range connections is limited to $N = L^2$. Note that in (a) for $\alpha = d + 1 = 3$, δ_s decreases with L, while for other values of α, δ_s is roughly constant. In (c) for $\alpha = d + 1 = 3$, γ_s keeps roughly constant and for other values of α, γ_s increases with L. This suggests that for $\alpha = 3$ the relation between $\langle \ell \rangle$ and L is a function that increases less than a power law and more likely that $\langle \ell \rangle$ increases logarithmically with L.

bound $\langle \ell \rangle$ by the relation $\langle \ell \rangle > \rho^{-1/d}$. Here $\rho^{-1/d}$ is from the small-world model in which $\alpha = 0$, with a fixed concentration of links $\langle \ell \rangle \sim \rho^{-1/d} \ln L$ [39]. Since, for $0 < \alpha < d + 1$, $\langle \ell \rangle$ decreases with increasing α, the bound $\langle \ell \rangle > L^{(d+1-\alpha)/d}$ is rigorous and $\langle \ell \rangle$ in this range must scale as a power of L. For $\alpha > d + 1$ and $N \to \infty$, from Eq. (6) $\langle r \rangle \sim 1$ and the density becomes independent of the system size, i.e., $\rho \sim 1$. When this is the case, the effect of the constraint Λ on navigation is negligible. Thus the navigation on the networks is similar to the original lattice without additional long-range connections; therefore $\langle \ell \rangle \sim L$. Thus we conclude that, as Figs. 5(b)–5(d) show, when $\alpha = d + 1$, the increase with L of $\langle \ell \rangle$ is less rapid than a power law and may scale logarithmically with L.

VI. SUMMARY

We analyzed the navigation with global knowledge (knowing the shortest path between any two sites) in d-dimensional lattices. We assumed additional long-range links following a power-law distribution $p(r) \sim r^{-\alpha}$ with the total length constraint proportional to system size L^d. Our results suggest that the optimal navigation is obtained when the exponent $\alpha = d + 1$ for one-, two-, and three-dimensional lattices and $\alpha = d_f + 1$ for fractal lattices. This result can be compared to the optimal local navigation without cost constraint found by Kleinberg [25] to be for $\alpha = d$. In the situation when α is near the critical threshold, the structure of the long-range connections form a type of gradient that the whole network reaches the optimal navigation and below this critical value the network becomes more homogeneous. While with the condition that the total cost is constrained, the critical threshold is shifted to $d + 1$ because the network reaches a new state in which the heterogeneity of the length of connections is maximized at this new critical point under the competitive equilibrium between the length and number of long-range connections. We also found that in the optimal condition ($\alpha = d + 1$), the number of nodes needed to have long-range links is extremely low and represents a zero fraction of the total number of nodes. We also studied the scaling of the shortest path $\langle \ell \rangle$ with L and found that while for $\alpha \neq d + 1$ the scaling is a power law with L, for $\alpha = d + 1$ the scaling is of logarithmic dependence on L (except for $d = 1$).

ACKNOWLEDGMENTS

We wish to thank NSF (Grant No. CMMI 1125290), ONR (Grants No. N00014-09-1-0380, and No. N00014-12-1-0548), DTRA (Grants No. HDTRA-1-10-1-0014, and No. HDTRA-1-09-1-0035), the European EPIWORK, MULTIPLEX, CONGAS (Grant No. FP7-ICT-2011-8-317672) and LINC projects, DFG, the Next Generation Infrastructure (Bsik) and the Israel Science Foundation for financial support. We also thank to the Brazilian Agencies CNPq, CAPES, FUNCAP, and FINEP, the FUNCAP/CNPq Pronex grant, and the National Institute of Science and Technology for Complex Systems in Brazil.

[1] R. Albert and A.-L. Barabási, Rev. Mod. Phys. **74**, 47 (2002).
[2] M. E. J. Newman, SIAM Rev. **45**, 2 (2003).
[3] S. N. Dorogovtsev and J. F. F. Mendes, *Evolution of Networks: From Biological Nets to the Internet and WWW* (Oxford University Press, Oxford, 2003).
[4] R. Pastor-Satorras and A. Vespignani, *Structure and Evolution of the Internet: A Statistical Physics Approach* (Cambridge University Press, Cambridge, 2004).
[5] G. Caldarelli and A. Vespignani, *Large Scale Structure and Dynamics of Complex Webs* (World Scientific, Singapore, 2007).
[6] M. E. J. Newman, *Networks: An Introduction* (Oxford University Press, Oxford, 2010).
[7] R. Cohen and S. Havlin, *Complex Network: Structure, Robustness and Function* (Cambridge University Press, Cambridge, 2010)
[8] P. Erdős and A. Rényi, Publicationes Mathematicae Debrecen **6**, 290 (1959).
[9] P. Erdős and A. Rényi, Publications of the Mathematical Institute of the Hungarian Academy of Sciences **5**, 17 (1960).
[10] S. Milgram, Psychol. Today **2**, 60 (1967).
[11] D. J. Watts and S. H. Strogatz, Nature (London) **393**, 440 (1998).
[12] D. J. Watts, *Small Worlds: The Dynamics of Networks between Order and Randomness* (Princeton University, Princeton, 1999).
[13] A.-L. Barabási and R. Albert, Science **286**, 509 (1999).
[14] M. Barthélemy, Phys. Rep. **499**, 1 (2010).
[15] P. Expert, T. S. Evans, V. D. Blondel, and R. Lambiotte, Proc. Natl. Acad. Sci. USA **108**, 7663 (2010).
[16] D. Li, K. Kosmidis, A. Bunde, and S. Havlin, Nat. Phys. **7**, 481 (2011).
[17] W. Li, A. Bashan, S. V. Buldyrev, H. E. Stanley, and S. Havlin, Phys. Rev. Lett. **108**, 228702 (2012); A. Bashan, Y. Berezin, S. V. Buldyrev, and S. Havlin, arXiv:1206.2062v1.
[18] C. M. Schneider, A. A. Moreira, J. S. Andrade, Jr., S. Havlin, and H. J. Herrmann, Proc. Natl. Acad. Sci. USA **108**, 3838 (2011).
[19] G. Bianconi, P. Pin, and M. Marsili, Proc. Natl. Acad. Sci. USA **106**, 11433 (2009).
[20] M. P. Viana and L. da F. Costa, Phys. Lett. A **375**, 1626 (2011).
[21] P. A. Morais, J. S. Andrade, E. M. Nascimento, and M. L. Lyra, Phys. Rev. E **84**, 041110 (2011).
[22] H.-X. Yang, W.-X. Wang, Y.-B. Xie, Y.-C. Lai, and B.-H. Wang, Phys. Rev. E **83**, 016102 (2011).
[23] L. K. Gallos, H. A. Makse, and M. Sigman, Proc. Natl. Acad. Sci. USA **109**, 2825 (2012).
[24] L. K. Gallos, H. A. Makse, and M. Sigman, Front. Physiol. **3**, 123 (2012).
[25] J. M. Kleinberg, Nature (London) **406**, 845 (2000).
[26] M. R. Roberson and D. Ben-Avraham, Phys. Rev. E **74**, 017101 (2006).
[27] G. Li, S. D. S. Reis, A. A. Moreira, S. Havlin, H. E. Stanley, and J. S. Andrade, Phys. Rev. Lett. **104**, 018701 (2010).

[28] K. Kosmidis, S. Havlin, and A. Bunde, Europhys. Lett. **82**, 48005 (2008).
[29] H. Yang, Y. Nie, A. Zeng, Y. Fan, Y. Hu, and Z. Di, Europhys. Lett. **89**, 58002 (2010).
[30] Y. Li, D. Zhou, Y. Hu, J. Zhang, and Z. Di, Europhys. Lett. **92**, 58002 (2010).
[31] Y. Hu, Y. Wang, D. Li, S. Havlin, and Z. Di, Phys. Rev. Lett. **106**, 108701 (2011).
[32] D. Li, G. Li, K. Kosmidis, H. E. Stanley, A. Bunde, and S. Havlin, Europhys. Lett. **93**, 68004 (2011).
[33] S. D. S. Reis, A. A. Moreira, and J. S. Andrade, Phys. Rev. E **85**, 041112 (2012).
[34] T. Emmerich, A. Bunde, S. Havlin, G. Li, and D. Li, Phys. Rev. E **87**, 032802 (2013).
[35] H. Youn, M. T. Gastner, and H. Jeong, Phys. Rev. Lett. **101**, 128701 (2008).
[36] D. Stauffer and A. Aharony, *Introduction to Percolation Theory* (Taylor & Francis, London, 1992).
[37] A. Bunde and S. Havlin, *Fractals and Disordered Systems* (Springer, Heidelberg, 1995).
[38] B. B. Mandelbrot, *Fractals: Form, Chance and Dimension* (Freeman, San Francisco, 1977).
[39] M. Barthélémy and L. A. N. Amaral, Phys. Rev. Lett. **82**, 15 (1999).